Journal of Materials Science: Materials in Engineering

ORIGINAL PAPER Open Access

Modeling and numerical simulation of car frontal crash test using finite element method

Driss Bendjaballah[1], Mohamed Sahli[2*] and Thierry Barrière[3]

Abstract

Nowadays, the development of safety systems for passenger protection in the automotive industry relies heavily on numerical simulations. FE simulation was widely used to study the sensitivity of design parameters and their influence on costs and/or overall weight in new car models through the inspection of different scenarios developed. In this article, crash simulations were conducted to simulate a car accident via the finite element method. The aim was to analyze the performance of a car structure deforming during the collision in the presence of dummy, belted or not, to determine the degree of safety provided to the occupants of the car. The CAD model of the car and the dummy was made using LS-DYNA software; the collision impulse of the vehicle and the speed of the driver's seat were observed and compared. Various incoming speeds were taken into account when the car was modeled to crash into a wall.

Keywords Crashworthiness, LS-DYNA, Deformation, FE analysis, Airbag

Introduction

Recent years were marked by a large increase in the number of vehicle accidents, mainly in head-on situations, and the resulting serious injuries. Indeed, these accidents increasingly constitute a burden on public health, particularly in low-income countries (Abdullah et al. 2020; Gong et al. 2021; Zhang et al. 2018; Frej et al. 2021). This was why many car manufacturers were focused on this problem and tried to solve it through the different safety devices integrated into the cabin of their cars in order to mainly improve the driver and passenger's safety, in particular energy-absorbing steering columns, side and rear airbags, and impact beams in the side doors, among others (Fathalla et al. 2022; Mei and Thole 2008).

Although car crash tests were necessary to evaluate vehicle-level safety, the expenses directly related to these tests were too expensive and the test result was not always stable due to random factors, which drastically limits the crash tests number (Lu et al. 2021; Idrees et al. 2023).

Consequently, numerical methods have established themselves as one of the most widespread methods for addressing this type of problem (Mazurkiewicz et al. 2018; Baranowski et al. 2018; Klasztorny et al. 2016; Ratajczak et al. 2017; Arkusz et al. 2019). Numerical simulations make it possible to quickly evaluate the structure in order to verify and validate its conformity and to predict its behavior in different scenarios with the advantage of making significant savings (Mazurkiewicz et al. 2018; Joszko et al. 2016).

These simulations can also be used to assess the safety of the driver and passengers, help reduce the cost of real-world crash tests, and can also play a very instrumental role in the development of new vehicles and help reduce the risk of crashes. A car collision in the shorter term

*Correspondence:
Mohamed Sahli
sahlisofiane2@yahoo.fr
[1] Mechanical Laboratory, Mechanical Engineering Department, Faculty of Science of Technology, University Frères Mentouri, 25000 Constantine, Algeria
[2] ENSICAEN, UNICAEN, CEA, CNRS, CIMAP, Normandie University, 14000 Caen, France
[3] Institut FEMTO-ST, National Centre for Scientific Research (CNRS), University of Franche-Comté, 25000 Besancon, France

and at lower cost (Kwasniewski et al. 2009; Danek and Gąsiorek 2018; Burkacki et al. 2020; Jedliński et al. 2020). A real-life case of a vehicle traveling during a head-on collision at approximately 100 km/h is shown in Fig. 1 below.

Before the development of powerful computers suitable for crash test simulations, automobile manufacturers relied exclusively on purely experimental large-scale tests. However, these tests were very expensive, time consuming, and essentially required sophisticated infrastructure and highly trained personnel. Therefore, multiphysics modeling and numerical simulation became increasingly widely used with the ultimate goal of studying and analyzing car accidents. Some researchers were working on how to establish a data-driven approach to car crash analysis. They worked on finite element models to analyze the differences in car accident scenarios. Safari et al. (2017) simulated a frontal and side impact with roof crushing for a Dodge Neon type vehicle in order to evaluate the structural resistance to this impact type. They ultimately showed that Advanced High Strength Steel materials, due to their excellent properties, were considerable potential for assessing the safety performance of a vehicle in the collision event (Patil Sagar and Patil 2021). Qi et al. (2006) carried out a frontal impact simulation for a commercial vehicle. They showed that by changing the material and structure types of the automobile's front casing, the energy absorption capacity was significantly improved (Safari et al. 2017). Marler et al. (2006) developed a FE model to study a commercial vehicle frontal collision using a multi-objective optimization approach. The front of the vehicle was modeled as a 3 DOF system consisting of the passenger compartment, the front wheels, crossmember, suspension system, and motor connected together by springs (Qi et al. 2006). Klausen et al. (2014) introduced a firefly optimization method to estimate vehicle crash test parameters based on a single mass-spring-damper model (Marler et al. 2006; Klausen et al. 2014). Ofochebe et al. (2015) studied the performance of a vehicle front structure using a 5-degree-of-freedom lumped mass-spring model consisting of the body, engine, crossmember, suspension, and bumper masses (Klausen et al. 2015). Gabler et al. (2000) developed LPMs for vehicle-to-barrier and vehicle-to-vehicle collisions using the SISAME code to extract model parameters (Ofochebe et al. 2015). Recently, Mazurkiewicz et al. (2018) also used LPM to improve the safety of children transported in vehicles subjected to a side impact during a vehicle accident (Gabler et al. 2000). Vangi et al. (2018) proposed a step-by-step procedure to collect data for a reconstruction of a two-vehicle accident (Mazurkiewicz et al. 2018). Teng et al. (2008) examined the dynamic response of a human body during an accident and assessed injuries sustained to the head, chest, and pelvic regions of the occupant (Vangi et al. 2018). Li et al. (2015) quantitatively estimated occupant injuries in automobile accidents. They used occupant injury criteria based directly on fictitious responses and compared them to those based solely on vehicle responses (Teng et al. 2008). The impact resistance of the side doors and the B-pillar in a side-pillar impact test was also evaluated by Lilehkoohi et al. (2014). The results show that to increase the amount of energy absorbed, it was necessary to take greater account of the part that had the most influence on the vehicle's impact resistance (Li et al. 2015).

In this article, we virtually simulated a car collision to understand the devastating consequences that car accidents can have on passengers. To simplify the study, only the vehicle's chassis with the driver was taken into account in our studies. The car model and mannequins were generated in Solidworks 3D modeling software and then imported into Lsdyna FEM analysis software for

Fig. 1 Frontal crash of a vehicle at a speed around 100 km/h. Data taken from Ref. (Tabiei and Wu 2000)

mesh generation and FEM analysis. The wall was therefore not modeled in our studies.

Numerical simulation description of the crash test

In our developed FE model, great emphasis was placed on considering only the key elements of vehicle safety systems that could influence passenger behavior during a frontal collision. Therefore, it was decided to model only a section of the vehicle and give it the properties of a rigid structure. The deformable seat, windshield, dashboard, and seat belt were modeled inside the car (see Fig. 2).

The FE LS-DYNA software was used to simulate a frontal collision of a vehicle model with an adult driver wearing a belt and traveling at a speed greater than or equal to 40 km/h. This will allow us to understand the traumatic mechanisms involved in accidents. The CAD of the car (bumper, chassis, hood, windshield and roof) and the models were made using Solidworks software, then discretized using LS-DYNA software. However, in this case, explicit LS-DYNA must be used due to the highly nonlinear transient dynamics phenomenon during crash tests. The meshes of the mannequins and the vehicle were meshed separately and then assembled, and the complete model includes in total more than 111 components, 54,000 elements, and 11,060 nodes (see Fig. 2). The simulation contained several contact definitions, comprising several contact pairs. Two contact types implemented in LS-DYNA (Lilehkoohi et al. 2014; Hallquist 2006; Ls-Dyna and R8.0 keyword user's manual 2015) were used: an automatic single-surface contact and an automatic surface-to-surface contact. The first was the automatic single-surface contact SOFT = 1 for the vehicle, with the following specified friction coefficients: fs = 0.3 and $f_d = 0.2$, where f_s was the static friction coefficient and f_d was the dynamic friction coefficient. Then, there was the automatic surface-to-surface contact SOFT = 2 for the vehicle's airbag with friction coefficients of $f_s = 0.9$ and $f_d = 0.8$. Finally, another automatic surface-to-surface contact SOFT = 1 was introduced to account for the friction between the vehicle and the dummy, with coefficients of $f_s = 0.45$ and $f_d = 0.315$. The friction coefficients for various materials were set on the basis of previous literature (Bielenberg et al. 2014; Wilde et al. 2019; Baranowski et al. 2007; Reid et al. 2007; Gutowski et al. 2017) and several preliminary parametric studies.

The theoretical background and results of the two materials that can be used to model the mechanical behavior of the seat belt and the airbag are shown (Gutowski et al. 2017; Bendjaballah et al. 2017a).

The simulations were carried out in a standard shock configuration with a rigid and fixed obstacle. The obstacle was hit by the front of a vehicle at different speeds between 40 km/h and 90 km/h.

Experimental set-ups and identification methodology

The deformation due to the crash can be taken into account in the simulation via several behavior laws whose parameters are to be identified and then validated by experimental tests to be set up. In our study, the Johnson–Cook model is used (Bendjaballah et al. 2017b).

$$\sigma = (A + B\varepsilon^{\eta})\left[1 + C\ln\left(\frac{\dot{\varepsilon}}{\dot{\varepsilon}_0}\right)\right]\left[1 - \left(\frac{T - T_r}{T_m - T_r}\right)^m\right]$$

In this equation, A, B, and C are the initial yield stress, strain hardening coefficient and reference strain rate coefficient, n is the strain hardening exponent, ε_γ is the rate of plastic strain. The thermal softening parameter is denoted by m.

Tensile tests were carried out on the MTS universal tensile machine at the mechanical testing laboratory of the University of Constantine (Algeria) to determine the thermophysical properties of several elements such as

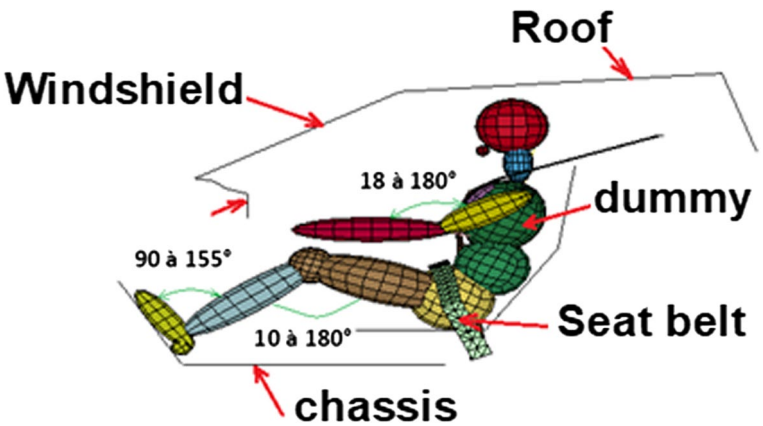

Fig. 2 Finite element model used in the numerical simulation of a frontal collision (Bendjaballah et al. 2017a)

the seat belt, the mannequin, and the metal chair stands. They were also used to identify the behavioral law parameters used to develop our simulation model.

The material chosen for the car parts, such as the bumper, is AISI 304L steel, which is the most widely used among all steels due to its weldability and excellent toughness. Then, the chassis cover and the roof used AA5052 aluminum for its lightness, excellent mechanical characteristics, and recyclability. Finally, the car's dashboard and windshield were supposed to be made of polypropylene and glass, respectively. The mechanical properties of the materials are related in Table 1.

Different samples were cut according to certain standards from the base material. These tests were conducted at a crosshead speed of 1 mm/min using max 100 kN. Each tensile test for a given material was conducted on five samples at room temperature. Axial force and displacement acquired during a tensile test are converted into stress and strain and continuous recording of tensile stress–strain tests was carried out during the loading and unloading phases (see Fig. 3).

The Johnson-Cook model parameters for AA5052 and AISI 304L are listed in Table 2. The fitness function of the genetic algorithm is obtained from the least squares principle as follows (Johnson and Cook 2018):

Table 1 Comparison of properties between AL-AA5052 and other materials

Materials	Density [kg/m^3]	Elasticity modulus [GPa]	Yield stress [MPa]	Poisson's ratio	Elongation at break [%]
AA5052	2700	69	320	0.34	10
AISI 304L	7800	210	340	0.29	15
PP plastic	1400	1.6	14	0.40	300
Glass	2230	69	80	0.30	3
Polyester	1200	10.6	8.3	0.38	2.5

Table 2 Johnson–Cook strength model parameters for AA5052 and AISI 304L

Parameters	Values	
	AA5052	AISI 304L
Initial yield stress A	176.6	239
Hardening constant B	289.4	522
Hardening exponent N	0.3712	0.65
Strain rate constant C	0.001	0.02
Thermal softening exponent m	1	1
Reference strain rate (/sec)	1	1

N represents the experimental groups number, $k1$ refers to a proportionality constant value − 1, and i expresses the experimental sequence number.

At the end of the identification process, a set of parameters was determined and then validated through a comparative study between tensile tests and the modeling of the constitutive laws used in this study (see Table 2). For monotonic tensile loadings, both experimental and modeling approaches provide fairly similar responses in terms of stress evolution versus function of strain, with better prediction in the elastic part. However, we can therefore admit that these results are valid (see Fig. 4).

Numerical results and discussions

Frontal impact at 40 Km/h

The behavior response of the belted driver during a frontal collision was illustrated in Fig. 5. After 20 ms, the dummy's back begins to leave the seat back and move forward with the neck slightly bent; when the time is 40 ms, the mannequin continues to move forward, the head tends to lower, the arms move forward, and the legs also begin to flex. During the collision, the entire dummy slides forward along the seat, the head lowers, the arms continue to move forward, and the

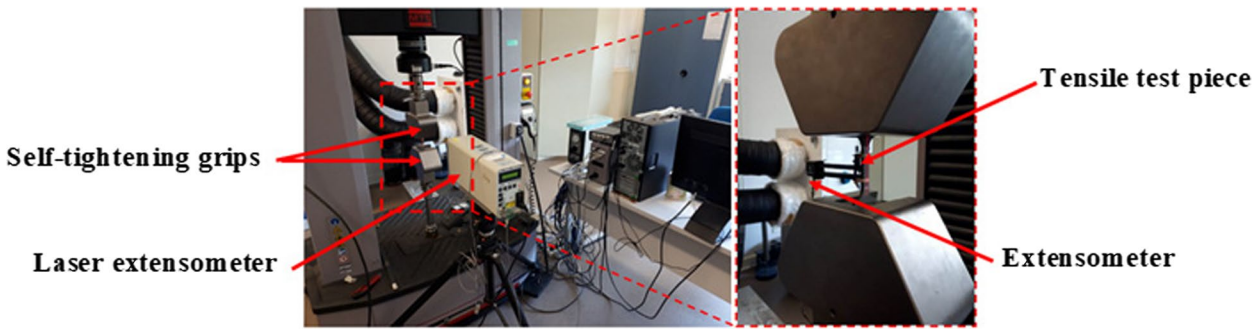

Fig. 3 A photograph of MTS universal testing

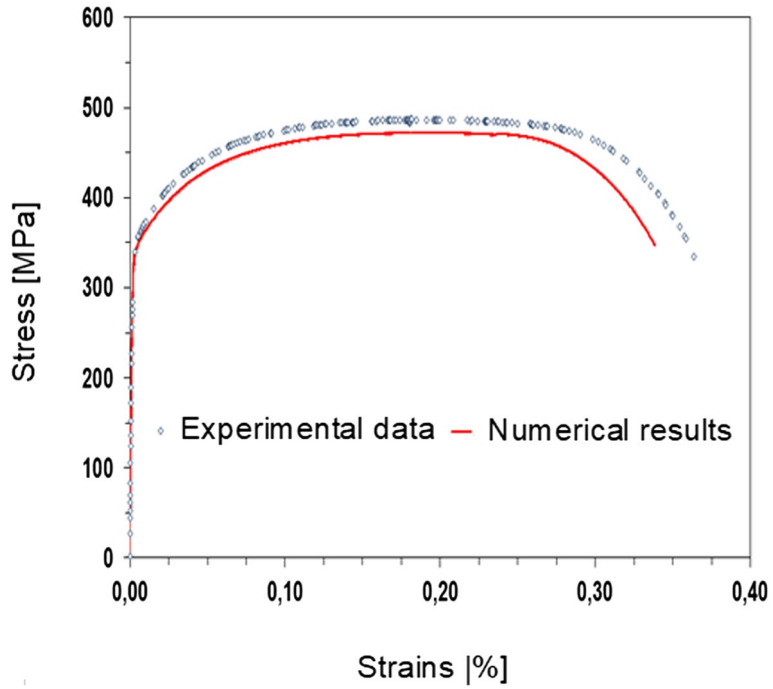

Fig. 4 Comparison of results between experimental and simulation at room temperature in the rolling direction of a DP steel specimen

legs bend with greater amplitude. At 40 km/h, the car undergoes the least deformation compared to the last two cases.

Frontal impact at 70 km/h

Figure 6 shows the driver's behavior at the moment of impact obtained at 70 km/h. The results of the study show that the user does not directly interact with the interior of the vehicle during the collision. Thanks to the seat belt, the driver was held securely in his seat after a collision. The movement of the drive's body was extremely safe for himself and other road users who collide head-on with the driver. We can first observe that the seat belt tightens so as to keep the body attached to the seat (see Fig. 6). It was therefore a key element to guarantee the protection of the driver in the event of an impact since it absorbs a large part of the kinetic energy of a car during the collision, which therefore increases the safety of the occupants inside the vehicle.

Similar results were reported in Sybilski's study (L. Wang YCao., Z. Bai,, et al. 2016). Concerning, for example, the maximum longitudinal displacement of the gravity center of the dummy was reached at different times in each case. It should be noted that at this point, the mannequin's posture differs depending on the speed used. In these cases, the forearms and arms are pushed outwards while keeping the hands within the steering wheel. Knees can hit elements in the space under the steering wheel.

Frontal impact at 90 km/h

The numerical results of the dynamic behavior of a fully belted driver made it possible to record the driver's movements inside a tourist vehicle. Indeed, image sequences of a head-on collision at a speed of 90 km/h at different time intervals were shown in Fig. 7. It was noted that in none of the cases did the user go over or under the seat belt regardless of the impact speed imposed between 40 and 90 km/h. We also found that the driver's position and kinematics during the accident remained stable inside the cabin and secure at all times. Under these conditions, the results obtained make it possible to prove that the seat belt comfortably keeps the driver in place when seated, which generally increases their safety inside the vehicle. Additionally, the likelihood that the driver or passengers of the vehicle will suffer injury or serious injury during a traffic accident was greatly reduced when those passengers wear their seat belts properly.

Thus, these results also make it possible to see the speeds evolution of each component with maximum values recorded at the user's head. Indeed, in this situation, the only vulnerable part of the body was the

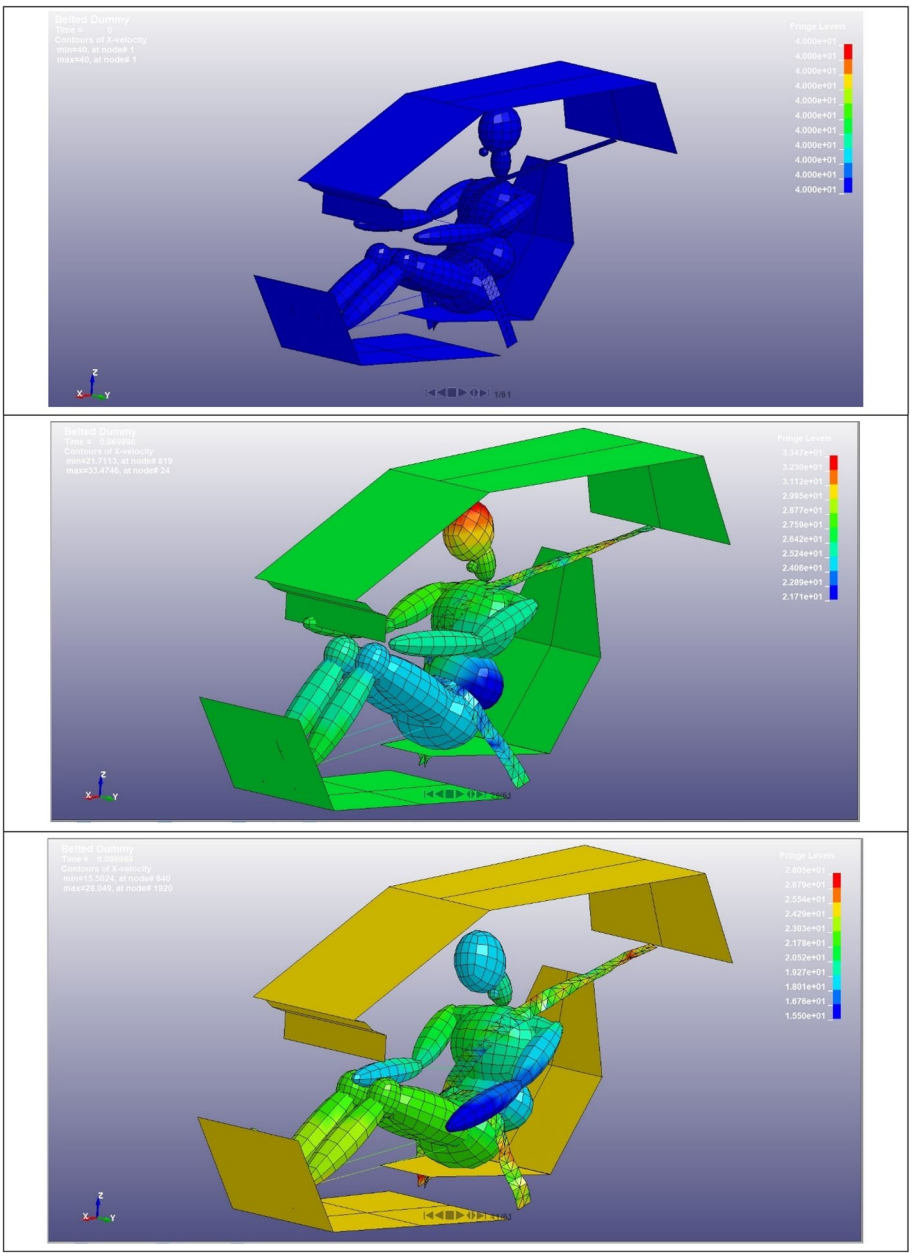

Fig. 5 Dynamic behavior of an adult driver obtained following a frontal collision at 40 km/h

driver's head. It leans strongly forward depending on the impact speed, with the risk at the end of a collision of being pushed quickly backwards. This movement of the head, called whiplash, can cause trauma ranging from muscle micro-tears to cervical fractures accompanied by a severed spinal cord. They can also lead to irreversible quadriplegia or even the death of the driver. At this point, we can conclude that the presence of the head restraint was also essential to protect both the neck and the head of the driver during a collision.

The analysis of the dummy response

The numerical simulation results of a frontal collision with a rigid non-deformable obstacle obtained at different impact speeds varying between 40 km/h and 90 km/h were illustrated in Figs. 8, 9, and 10. We can see that the movements of the driver's body had an identical overall appearance; only the inclination angle of the head, the torso, and the rotation angle of the upper part of the body differed depending on the impact speed. As an indication, for an impact speed of 90 km/h, the

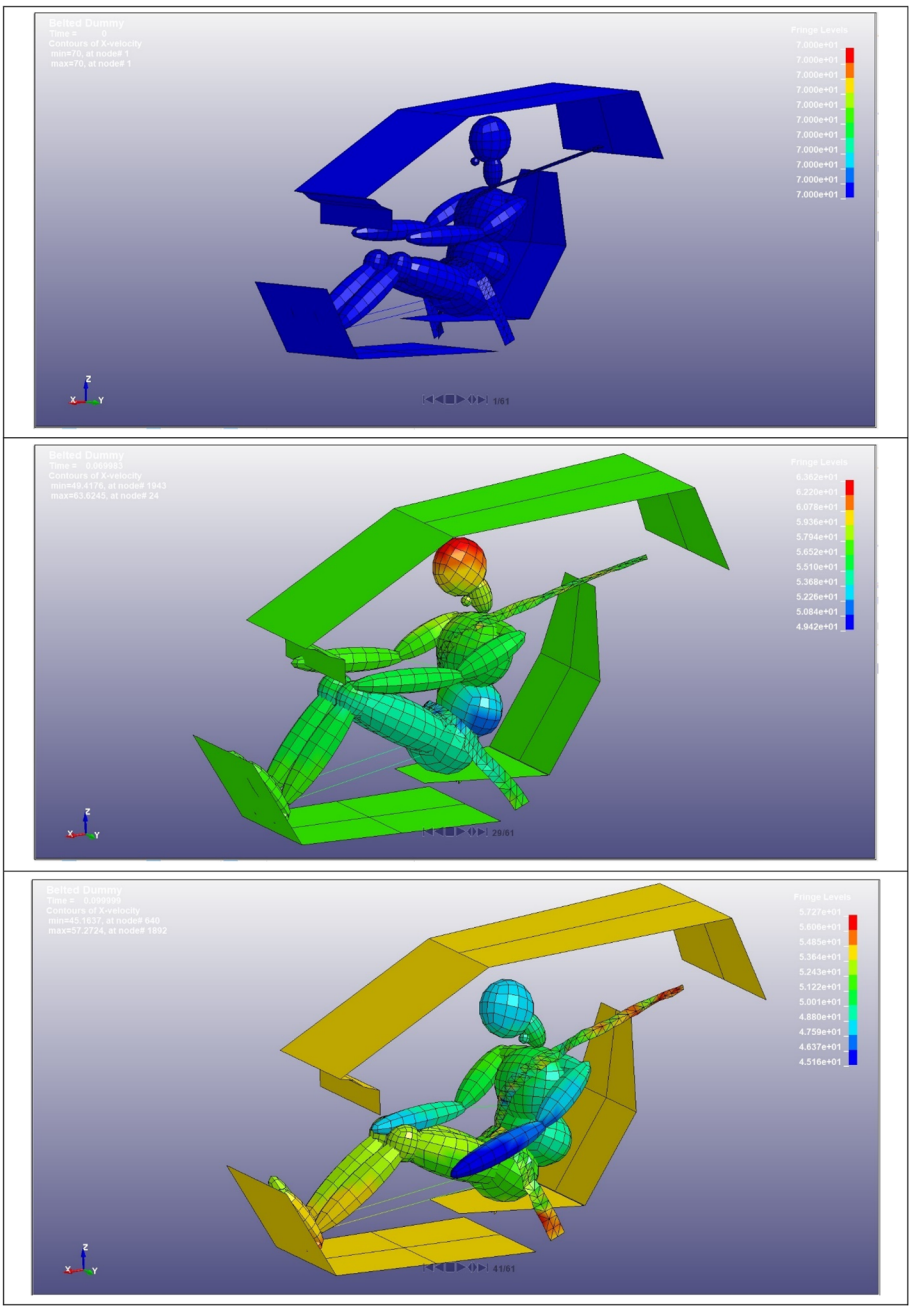

Fig. 6 Dynamic behavior of an adult driver obtained following a frontal collision at 70 km/h

inclination angle of the head and torso is equal to 33° and 37°, respectively. This phenomenon is naturally observed in real driving during a sudden frontal collision. At the moment of impact, it is accompanied by a forward separation of the driver's torso from the seat back. This is mainly due to the vehicle's inertia at the time of impact and the presence of the seat belt, which acts backward during this phase. Finally, the analysis showed that under the same conditions, the dynamic behavior of the driver was completely different for the case of a vulnerable or poorly belted user.

In the event of a frontal collision, both legs are generally extended forward or further back, each on a pedal. Seat belts, on the other hand, restrict the movement of the left arm, which naturally causes the driver's shoulders to rotate, as seen in Figs. 8, 9, and 10. This rotation usually increases when the torso begins to rest on the airbag. The lower limbs also play a major role in the collision,

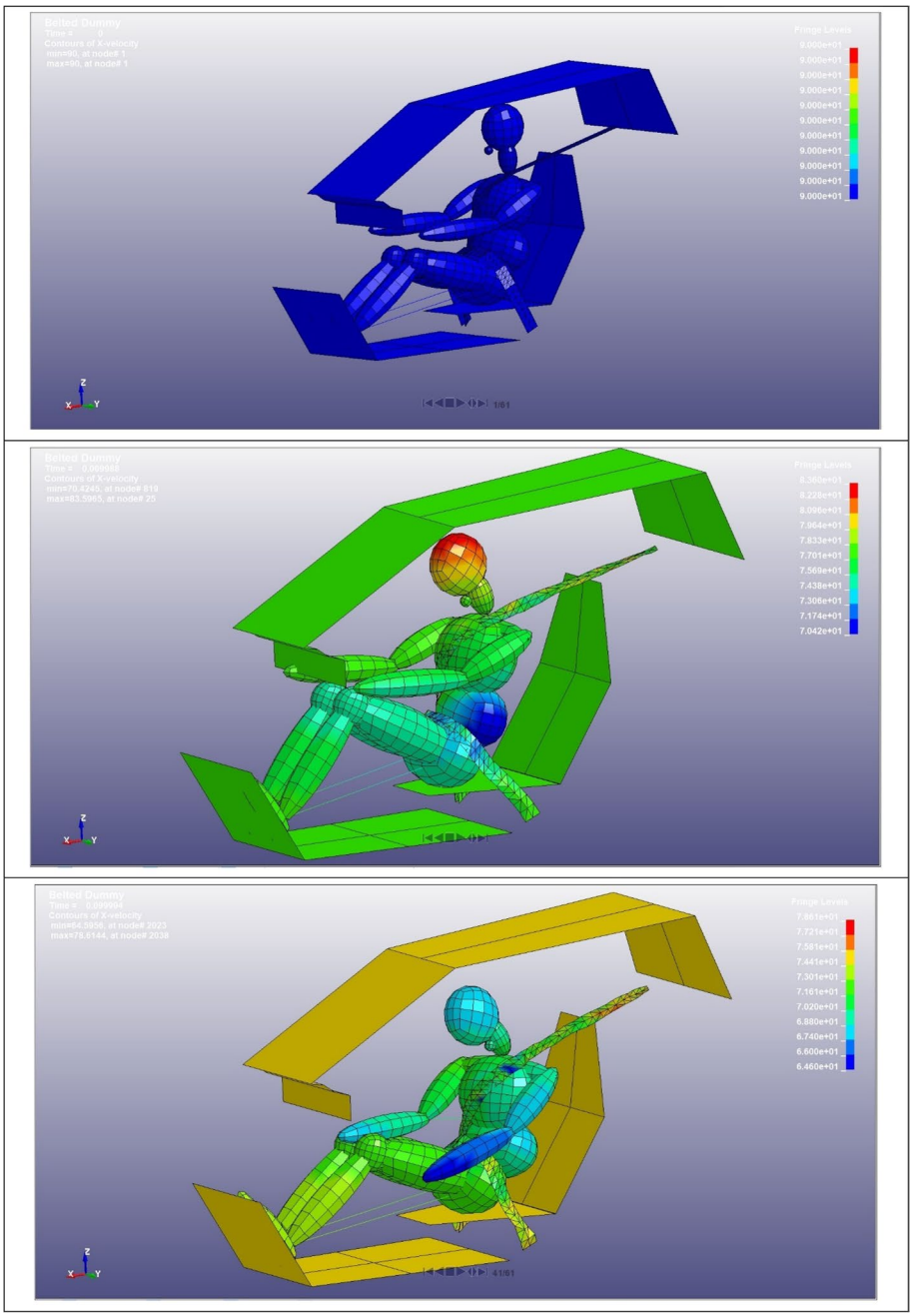

Fig. 7 Dynamic behavior of an adult driver obtained following a frontal collision at 90 km/h

as the driver moves primarily longitudinally towards the steering wheel, with the risk of the knees hitting the space under the steering wheel.

The impact speed used has a significant influence on the lateral displacement of the dummy's center of gravity. In the case of an impact at 90 km/h, the maximum displacement is approximately 15 mm located during the final phase of the impact. This lateral movement is accompanied by a maximum longitudinal displacement and shoulder rotation. Analyzing the numerical results, a significant change in shoulder rotation and also in the dummy's forward displacement is observed (see Fig. 8).

Collision speed has a significant impact on the driver's body position in terms of shoulder rotation, lateral displacement, and longitudinal displacement, which increases the risk of injury to vehicle passengers (see

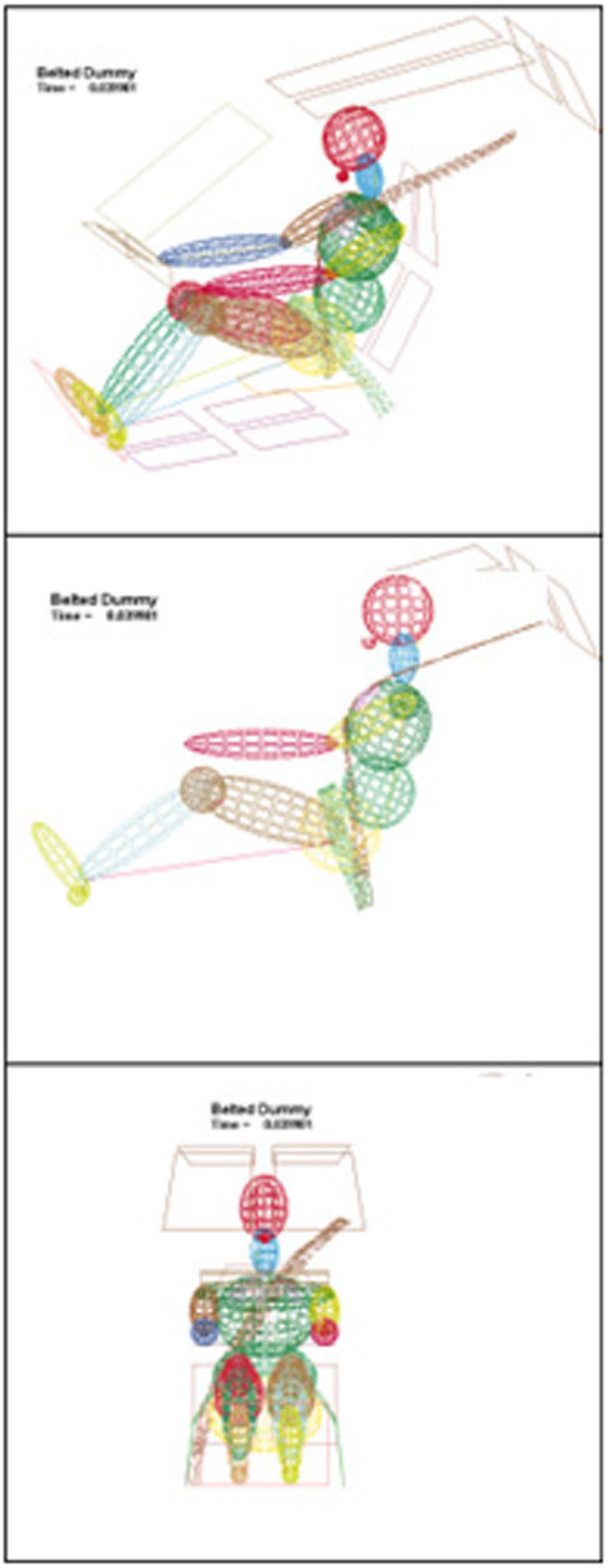

Fig. 8 Dummy response in the crash process—frontal impact at 40 km/h

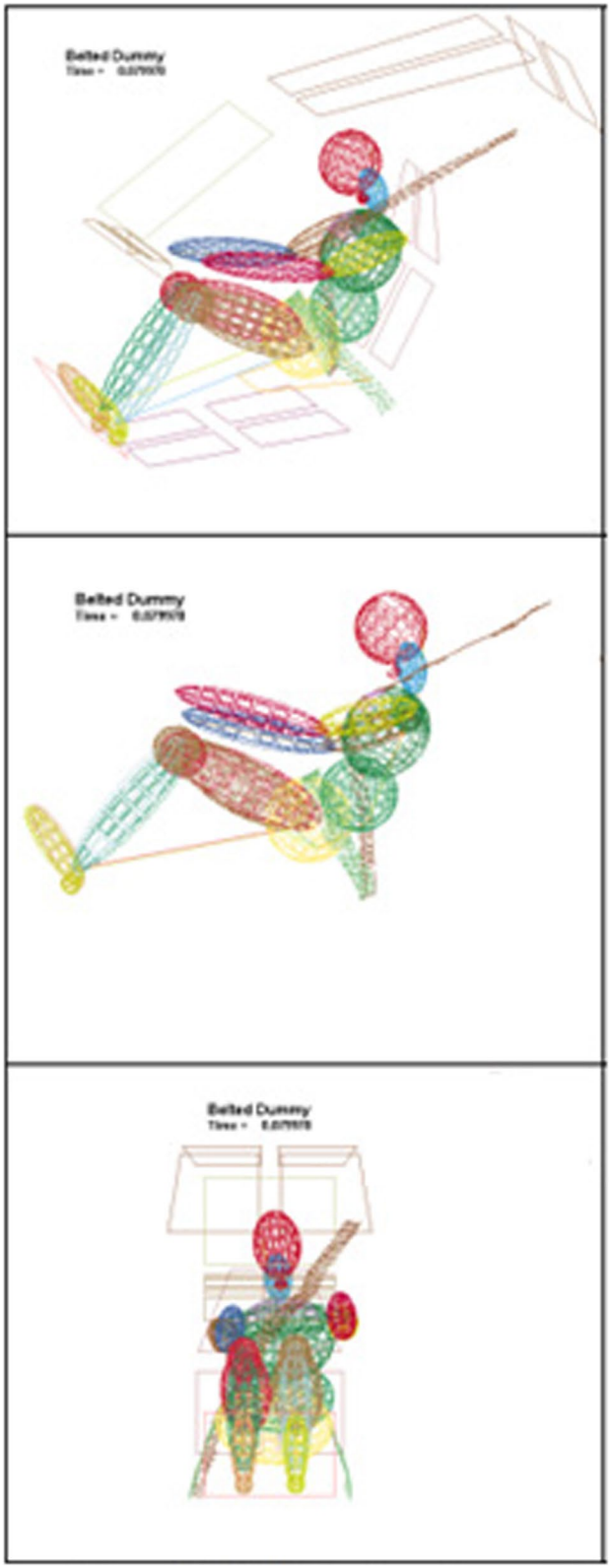

Fig. 9 Dummy response in the crash process—fontal impact at 70 km/h

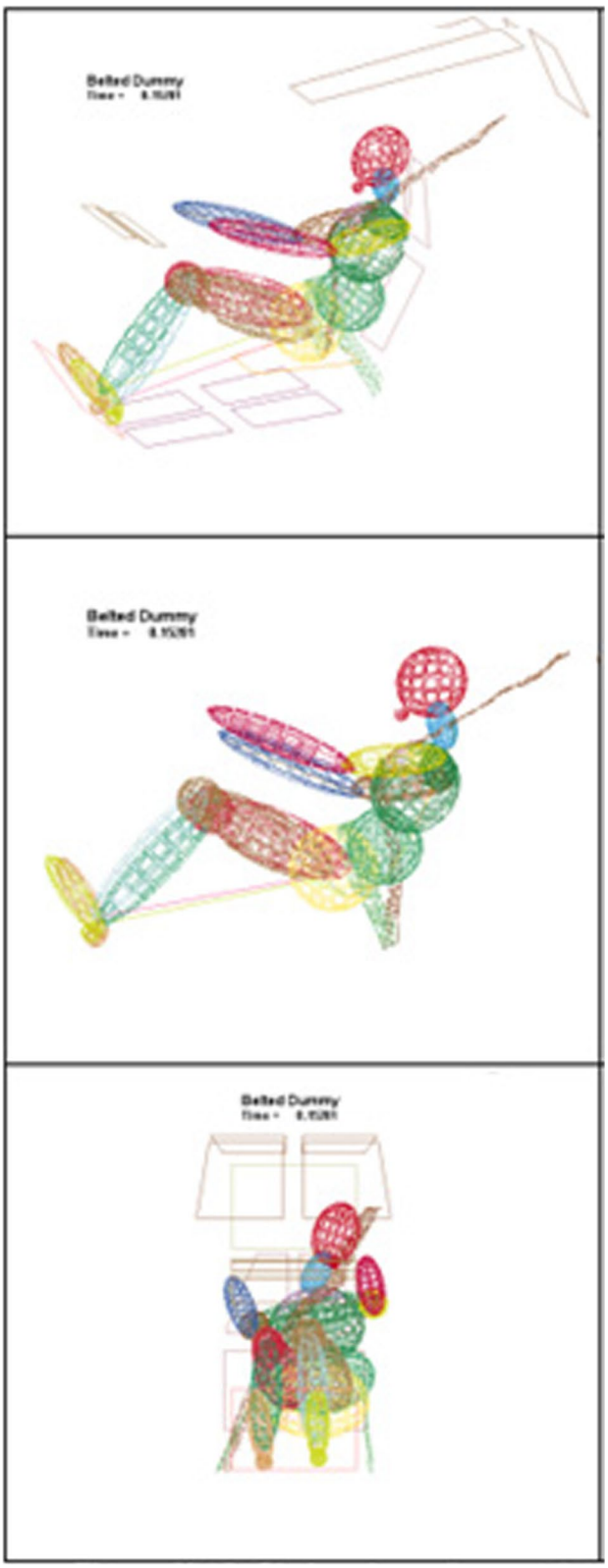

Fig. 10 Dummy response in the crash process—frontal impact at 90 km/h

Figs. 11, 12, and 13). During the collision, a back-and-forth shoulder movement was observed starting at 0.65 s. This phenomenon increases and reaches a maximum value of 9.2° around 0.75 s for a speed of 90 km/h. Compared to other collision speeds considered in this study, shoulder rotation decreased by between 21 and 23%. The same observations were also reported by (Pohlak, et al., 2007), (Sybilski and Małachowski 2021).

Regarding the driver's overall lateral displacement, a slight outward displacement was recorded at 0.74 s, which was in the order of 5 to 6 mm depending on the collision speed. It gradually increases for high collision speeds, i.e., 90 km/h, and becomes less significant for low speeds of around 40 km/h. In addition, a forward movement of the driver was also observed, which increased very quickly until reaching values of around 36.8 mm despite the presence of the seat belt.

Conclusions

In this study, a head-on collision of a vehicle at different speeds was simulated. These simulations were performed at different speeds using the Explicit Dynamics module of the ANSYS LS-DYNA version.

Firstly, thanks to the seat belt, the driver was held securely in his seat after a collision. Furthermore, the seat belt only constrains the upper torso and upper thighs and does not prevent forward movement of the head and neck. Rapid, violent movement of these areas of the body can cause muscle and ligament tearing and, in severe cases, can even lead to serious injury to the cervical spine.

Secondly, it was noted that in none of the cases did the user go over or under the seat belt regardless of the impact speed imposed between 40 and 90 km/h. The movement of the driver's body was extremely safe for himself and other road users who collide head-on with the driver. Under these conditions, the results obtained make it possible to prove that the seat belt comfortably keeps the driver in place when seated, which generally increases their safety inside the vehicle.

The results obtained by the simulation will soon be validated by comparison with the results of spit tests.

The final objective of the model developed after experimental validation will be to try to address different scenarios such as the effect of the position and/or the modification of the center of gravity of the passenger due to various physical disabilities, age and/or the modification of the body support points due to the use of several additional equipment to facilitate driving on the final behavior of the driver during a frontal collision. Given the impossibility of conducting such studies through

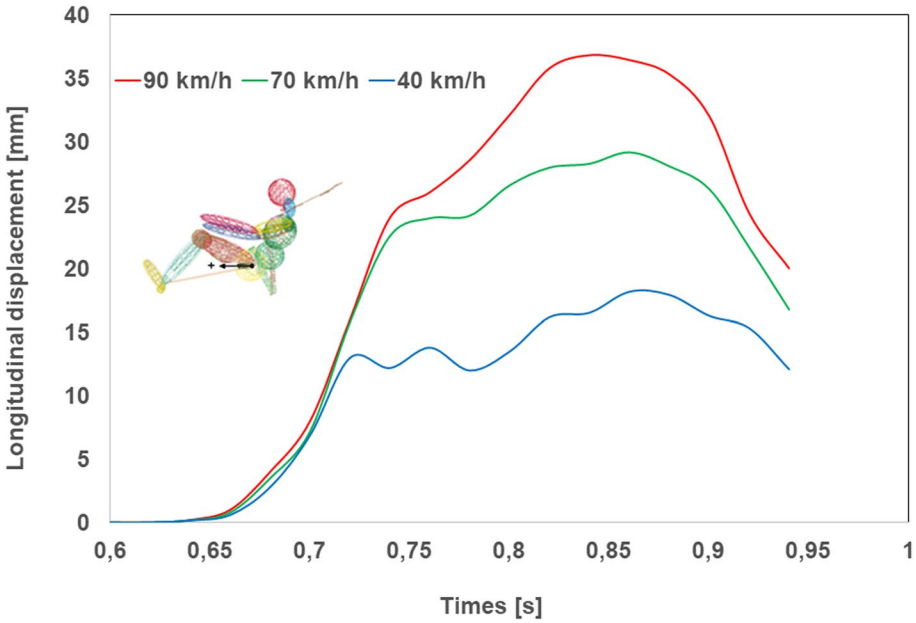

Fig. 11 Longitudinal displacement of dummy

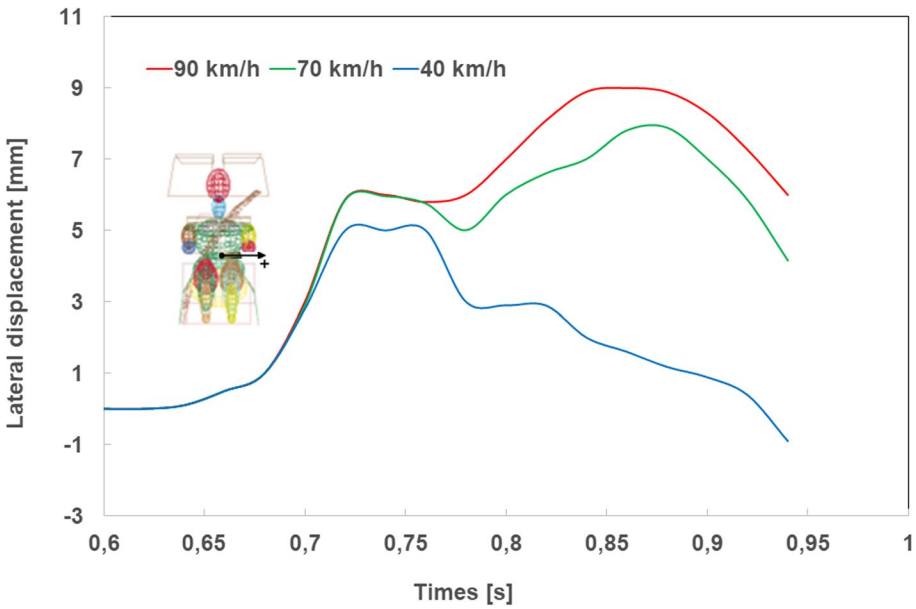

Fig. 12 Lateral displacement of dummy

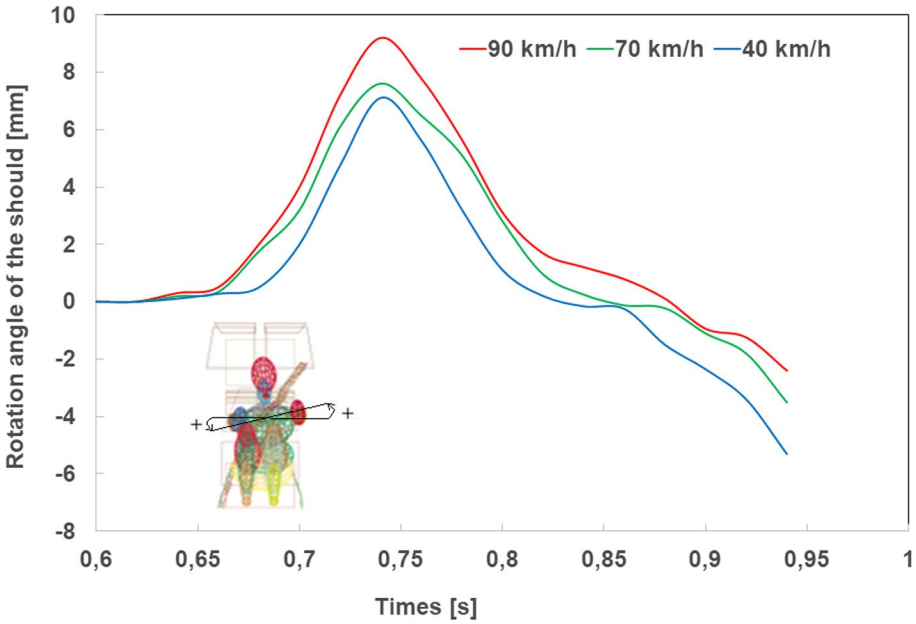

Fig. 13 Rotation angle of the shoulders

experimental tests, this is why great importance will soon be given to this aspect using our FE model.

Based on the results obtained, it is appropriate to conduct future research aimed at assessing passenger safety for people with disabilities or reduced mobility before a collision.

Author contributions

D. Bendjaballah has developed the EF model, performed the numerical simulations and carried out the implementation. He contributed to sample preparation and carried out with M. Sahli the experiment tensile tests. Us conceived and planned the experiments. D. Bendjaballah wrote the manuscript with support from M. Sahli and T. Barrière. M. Sahli and T. Barrière verified and valided the FE hypotheses methods, numericl results and supervised the findings of this work. All authors discussed the results, contributed to the interpretation of the results and to the final manuscript. Also, All authors provided critical feedback the manuscript and to the writing of the manuscript.

Declarations

Ethics approval and consent to participate

The authors of this article consent to the publication of this work in this journal and declare that they have complied with the ethics requirements.

Competing interests

The authors declare that they have no competing interests.

Received: 20 April 2025 Accepted: 24 July 2025
Published online: 26 August 2025

References

Abdullah NAZ, Sani MSM, Salwani MS, Husain NA (2020) A review on crashworthiness studies of crash box structure. Thin-Walled Structures 153:106795

Arkusz K, Klekiel T, Sławiński G, Będziński R (2019) Influence of energy absorbers on Malgaigne fracture mechanism in lumbar-pelvic system under vertical impact load. Comput Methods Biomech Biomed Engin 22:313–323

Baranowski P, Malachowski J, Janiszewski J, Wekezer J (2007) Detailed tyre FE modelling with multistage validation for dynamic analysis. Mater des 96:68–79

Baranowski P, Damaziak K, Mazurkiewicz L, Muszynski A, Vangi D (2018) Analysis of mechanics of side impact test defined in UN / ECE regulation 129. Traffic Inj Prev 19:256–263

Bendjaballah D, Bouchoucha A, Sahli ML, Gelin JC (2017) Numerical modelling and experimental analysis of the passenger side airbag deployment in out-of-position. Int J Crashworthiness. 22(5):527–40

Bendjaballah D, Bouchoucha A, Sahli M, Gelin J-C (2017b) Numerical analysis of side airbags deployment in out-of-position situations. International Journal of Mechanical and Materials. Engineering 12:2–9

Bielenberg RW, Faller RK, Reid JD, Schmidt JD, Pajouh MA Emerson E Development of retrofit, low-deflection portable concrete barrier system. J Transp Saf Secur. https://doi.org/10.1080/19439962.2017.1420717

Burkacki M, Wolański W, Suchoń S, Joszko K, Gzik-Zroska B, Sybilski K, Gzik M (2020) Finite element head model for the crew injury assessment in a light armoured vehicle. Acta Bioeng Biomech 22:174–183

Danek W, Gąsiorek D (2018) Numerical simulation of the car crash with aluminum, root mounted lighting column. Model Inżynierskie 35:25–30

Fathalla ASM et al (2022) A numerical study of the effect of bolt thread geometry on the load distribution of continuous threads. J Eng Res 10:158–173

Frej D, Podosek K, Kelvin T (2021) Overview of design solutions for child seats. Arch Automot Eng Arch Motoryz 92:33–47

Gabler HC, Hollowell W, Summers S. (2000) Systems modeling of frontal crash compatibility. In Proceedings of the 2000 SAE International Congress and Exposition, Detroit, MI, USA, 13–15 .pp 1–8.

Gong C, Bai Z, Wang Y, Zhang L (2021) On the crashworthiness performance of novel hierarchical multi-cell tubes under axial loading. Int J Mech Sci 206:106599. https://doi.org/10.1016/j.ijmecsci.2021.106599

Gutowski M, Palta E, Fang H (2017) Crash analysis and evaluation of vehicular impacts on W-beam guardrails placed behind curbs using finite element simulations. Adv Eng Softw 114:85–97

Hallquist JO (2006) LS-DYNA Theory Manual. Livermore Software Technology Corporation (LSTC), Livermor - California.

Idrees U, Ahmad S, Alam Shah I, Talha M, Shehzad R, Amjad M, Koloor S-SR (2023) Finite element analysis of car frame frontal crash using lightweight materials. J Eng Res 11:100007. https://doi.org/10.1016/j.jer.2023.100007

Jedliński T, Buśkiewicz J, Fritzkowski P (2020) Numerical and experimental analyses of a lighting pole in terms of passive safety of 100HE3 class. Vib Phys Syst 31:1–8
Johnson GR, Cook WA (2018) Constitutive model and data for metals subjected to large strains, high strain rates and high temperatures, Materials Science, Engineering.
Joszko K, Wolański W, Burkacki M, Suchoń S, Zielonka K, Muszyński A, Gzik M (2016) Biomechanical analysis of injuries of rally driver with head supporting device. Acta Bioeng Biomech 18:159–169
Klasztorny M, Nycz DB, Szurgott P (2016) Modelling and simulation of crash tests of N2-W4-A category safety road barrier in horizontal concave arc. Int J Crashworthiness 21:644–659
Klausen A, Tordal SS, Karimi HR, Robbersmyr KG, Jecmenica M, Melteig O (2014) Firefly Optimization and Mathematical Modeling of a Vehicle Crash Test Based on Single-Mass. J Appl Math 2014(1):150319. https://doi.org/10.1155/2014/150319.
Klausen A, Tørdal SS, Karimi HR, Robbersmy KG (2015) Mathematical modeling and numerical optimization of three vehicle crashes using a single-mass lumped parameter model. In Proceedings of the 24th International Technical Conference on the Enhanced Safety of Vehicles (ESV), Gothenburg, Sweden, 8–11 pp 44–49.
Kwasniewski L, Bojanowski C, Siervogel J, Wekezer JW, Cichocki K (2009) International Journal of Impact Engineering Crash and safety assessment program for paratransit buses. Int J Impact Eng 36:235–242
Li N, Fang H, Zhang C, Gutowski M, Palta E, Wang Q (2015) A numerical study of occupant responses and injuries in vehicular crashes into roadside barriers based on finite element simulations'. Adv Eng Softw 90:22–40
Lilehkoohi AH, Faieza AA, Sahari BB, Nuraini AA, Halali M (2014) Crashworthiness determination of side doors and b pillar of a vehicle subjected to pole side impact'. Applied Mechanics and Materials, Applied Mechanics and Materials 663:552–556
LSTC LS-DYNA R8.0 keyword user's manual (2015). https://ftp.lstc.com/anonymous/outgoing/web/ls-dyna_manuals/R15/LSDYNA_Manual_Volume_I_R15.pdf
Lu Y, Liu Y, Shu Y, Yin Y (2021) Injury prediction algorithm for rear-seat occupants in advanced automatic crash notification systems. IET Intelligent Transport Systems. 421–570. https://doi.org/10.1049/itr2.12153.
Marler RT, Kim CH, Arora JS (2006) System identification of simplified crash models using multi-objective optimization. Comput Methods Appl Mech Eng 195:4383–4395
Mazurkiewicz L, Baranowski P, Karimi HR, Damaziak K, Malachowski J, Muszynski A, Muszynski A, Robbersmyr KG, Vangi D (2018) Improved child-resistant system for better side impact protection. Int J Adv Manuf Technol 97:3925–3935
Mei L, Thole C-A (2008) Data analysis for parallel car-crash simulation results and model optimization. Simul Model Pract Theory 16:329–337
Ofochebe SM, Ozoegwu CG, Enibe SO (2015) Performance evaluation of vehicle front structure in crash energy management using lumped mass spring system. Adv Model Simul Eng 2:1–18
Patil Sagar S, Patil AV (2021) Analysis of frontal impact on a car after crash using FEA, International Journal of Advance Research and Innovation Idea in Education, ISSN(O)-2395–4396, 7;3096–3108.
Pohlak M, Majak J, Eerme M (2007) Optimization of car frontal protection system. Int J Simul Multidiscip Des Optim 1(1):31–37. https://doi.org/10.1051/ijsmdo:2007004
Qi W, Jin XL, Zhang XY (2006) Improvement of energy-absorbing structures of a commercial vehicle for crashworthiness using finite element method. Int J Adv Manuf Technol 30:1001–1009
Ratajczak M, Frątczak R, Sławiński G, Niezgoda T, Będziński R (2017) Biomechanical analysis of head injury caused by a charge explosion under an armored vehicle. Comput Assist Methods Eng Sci 24:3–15
Reid JD, Boesch DA, Bielenberg RW (2007) Detailed tire modeling for crash applications. Int J Crashworthiness 12:521–529
Safari H, Nahvi H, Esfahanian M (2017) Improving automotive crashworthiness using advanced high strength steels. Int J Crashworthiness. https://doi.org/10.1080/13588265.2017.1389624
Sybilski K, Małachowski J (2021) Impact of disabled driver's mass center location on biomechanical parameters during crash. Appl Sci 11(4):1427. https://doi.org/10.3390/app11041427
Tabiei A, Wu J (2000) Roadmap for crashworthiness finite element simulation of roadside safety structures. Finite Elem Anal des 34:145–157
Teng T, Chang F, Liu Y, Peng C (2008) Analysis of dynamic response of vehicle occupant in frontal crash using multibody dynamics method. Math Comput Model 48:1724–1736
Vangi D, Cialdai C, Gulino MS, Robbersmyr KG (2018) Vehicle accident databases: correctness checks for accident kinematic data. Designs 2:4
Wang L, Cao Y, Bai Z et al (2016) A parametric ribcage geometry model accounting for variations among the adult population. J Biomech. 49:2791–2798
Wilde K, Bruski D, Burzyński S, Chróścielewski J, Pachocki Ł (2019) LS-DYNA simulations of the impacts of a 38-ton heavy goods vehicle into a road cable barrier. In: 12 th European LS-DYNA conference. https://www.dynalook.com/conferences/12th-european-lsdyna-conference-2019/railway-and-commercial-vehicle/bruski_gdansk_university.pdf.
Zhang Y, Wang J, Chen T, Lu M, Jiang F (2018) On crashworthiness design of double conical structures under oblique load. Int J Vehicle Des 76:20–45.

Publisher's Note